

Glutamate Transporter Cluster Formation in Astrocytic Processes Regulates Glutamate Uptake Activity

Jianzheng Zhou and Margaret L. Sutherland

Department of Pharmacology, The George Washington University, Washington, DC 20037

Glutamate is the predominant excitatory neurotransmitter in the CNS, and it is removed from the synaptic cleft by sodium-dependent glutamate transport activity. Glutamate transporter-1 (GLT-1) is expressed predominantly in astroglial cells and is responsible for the largest proportion of glutamate transport in the adult forebrain. In the present study, we demonstrate the ability of endogenous and recombinant GLT-1 to form clusters in astrocytic processes and characterize the mobility and physiological importance of these clusters in the regulation of GLT-1 activity in the presence or absence of neurons. At the distal end of C6 glioma cell processes, GLT-1 clusters undergo rapid morphological changes in both shape and size, and these changes are inhibited by cytochalasin D treatment, suggesting that the morphogenesis of GLT-1 clusters is highly dependent on the actin network. Treatment of astrocytes with phorbol 12-myristate 13-acetate (PMA) quickly and preferentially decreases GLT-1 localization on the process membrane, leading to *de novo* generation of GLT-1 clusters along the process shaft. Pretreatment with the PKC inhibitor bisindolylmaleimide II (Bis II), with sucrose (0.4 M), or through the expression of a dominant-negative form of dynamin prevents PMA-induced GLT-1 internalization and cluster formation. In terms of glutamate transporter function, PMA treatment elicits a significant decrease in GLT-1 activity that is prevented by preexposure to either Bis II or hypertonic treatment. Together, these data indicate that GLT-1 trafficking and cluster formation in glial cell processes are dynamic events that play important roles in regulating glutamate uptake in astrocytes and glioma cells.

Key words: glutamate transport; astrocyte process; protein trafficking; GLT-1 cluster; glia; clathrin-dependent internalization

Introduction

Glutamate is the predominant excitatory neurotransmitter in the CNS (Fagg and Foster, 1983) and is removed from the synaptic cleft by a family of sodium-dependent glutamate transporters (Trotti, 2002). Glutamate transporters (GLTs) belong to a class of integral membrane proteins that contribute to sculpting EPSCs (Conti and Weinberg, 1999; Auger and Attwell, 2000) and are essential for maintaining physiological levels of glutamate (Tanaka et al., 1997). Of the five subtypes of glutamate transporters identified to date, GLT-1, localized almost exclusively to astrocytic processes (Conti and Weinberg, 1999), represents the predominant route for the clearance of extracellular glutamate in the adult forebrain (Sutherland et al., 1996; Robinson, 1998), and its functional inactivation raises extracellular glutamate to toxic levels (Rothstein et al., 1996; Tanaka et al., 1997).

It has been shown previously that GLT-1-positive puncta *in vivo* exclusively localize in astrocytic processes that highly overlap with the presynaptic marker synaptophysin (Minelli et al., 2001), raising the potential importance of GLT-1 clustering in the regulation of synaptic transmission. To date however, little is known about the basic characteristics of GLT-1 clustering in the astro-

cytic process and its physiological relevance. In the present study, by using green fluorescent protein (GFP)-tagged GLT-1, we define the dynamics of GLT-1 clustering in astrocytic processes and characterize its physiological importance in the regulation of GLT-1 activity.

Materials and Methods

Cell culture. Cortical astrocyte cultures and neuron–astrocyte cocultures were prepared from 1-d-old mice as described previously (Xu et al., 2003). To increase surface expression of GLT-1, astrocytic cultures were treated with dibutyryl-cAMP (dbcAMP) (150 μ M) for 7 d before experimentation. C6 glioma cells (American Type Culture Collection, Manassas, VA) were grown in DMEM supplemented with 10% fetal bovine serum, 2 mM glutamine, 100 U/ml penicillin, and 100 μ g/ml streptomycin.

cDNA constructs. A dominant-negative form of dynamin (K44A) was cloned into the pcDNA3 vector (Invitrogen, Carlsbad, CA). The mouse wild-type GLT-1 cDNA (Sutherland et al., 1995) was subcloned into pEGFP-N2 (Clontech, Palo Alto, CA) to create a fusion protein with GFP. C6 glioma cells were transfected with pEGFP–GLT-1 using FuGene 6 reagent (Roche, Indianapolis, IN), and stable transfectants were selected by growth in DMEM supplemented with 600 μ g/ml G418.

Measurement of Na⁺-dependent transport activity. Na⁺-dependent GLT-1 activity was measured as described previously (Hughes et al., 2004). Cells were grown on 24 well plates and rinsed twice with 1 ml of Krebs'–Ringer's–HEPES (KRH) solution before incubation with 50 nM [³H] D-aspartate in KRH buffer for 10 min. Na⁺-dependent uptake was defined as the difference between the signals observed in Na⁺-containing and choline-containing buffers.

Time-lapse visualization of GFP-tagged GLT-1. GLT-1–GFP-transfected astrocytes or C6 cells were cultured on glass-bottom cham-

Received Dec. 24, 2003; revised May 25, 2004; accepted May 25, 2004.

This work was supported by National Institute of Neurological Disorders and Stroke Grants NS41679 and NS42854.

Correspondence should be addressed to Dr. Margaret L. Sutherland, Department of Pharmacology, George Washington University, 2300 Eye Street Northwest, Washington, DC 20037. E-mail: phmmls@gwumc.edu.

DOI:10.1523/JNEUROSCI.1404-04.2004

Copyright © 2004 Society for Neuroscience 0270-6474/04/246301-06\$15.00/0

bers (LabTek-II, Ashland, MA). Real-time images were collected at room temperature and analyzed with OpenLab (version 3.14; Improvion, Lexington, MA). GLT-1 clusters are defined as a fluorescent area of >12 pixels with intensity at least four times higher than the background. Within a defined window, the average fluorescence intensity was determined for each time point captured to determine cluster size and number, as outlined above, using OpenLab software. To determine the preferential localization of GFP-tagged GLT-1, the ratios of fluorescence intensity in the membrane and adjacent cytoplasm were determined by directly measuring fluorescence with OpenLab software.

Biotinylation of cell-surface proteins and Western blot. The biotinylation procedure was performed as described previously (Xu et al., 2003). The biotinylated proteins were resolved on 10% SDS-polyacrylamide gels, transferred to nitrocellulose membrane, and probed with an N-terminal GLT-1-specific antibody (1:10,000; Invitrogen) for 1 hr. Proteins were visualized by enhanced chemiluminescence assay.

Results

GLT-1 clusters are mobile

It has been reported that GLT-1 mRNA and protein are greatly augmented in astrocyte–neuron cocultures (Schlag et al., 1998), demonstrating the importance of the cross-talk between astrocytes and neurons in regulating GLT-1 expression and distribution. In the present study, we examine the distribution of endogenously expressed GLT-1 in primary cultures of astrocytes treated with dbcAMP, which has been shown to speed astrocyte maturation and differentiation as well as elevate the level of GLT-1 protein in both the membrane and cytoplasm (Schlag et al., 1998). Immunocytochemical analysis of the dbcAMP-treated cultures demonstrates the uniform distribution of GFAP (Fig. 1*B*) throughout the cell. Endogenous GLT-1 (Fig. 1*A*) is also localized in the astrocytic membrane, cytoplasm, and processes. However, immunopositive GLT-1 puncta are found on the astrocytic processes with preferential localization at either the distal end or fork of the processes (Fig. 1*A,C*, arrowheads). In astrocytes and C6 cells transfected with the pEGFP–GLT-1 construct, GLT-1–GFP also forms clusters on the processes (Fig. 1*D,E*), similar to the endogenous transporter, with preferential localization at either the fork or the distal end of processes. This is in contrast to the distribution of GFP alone, which distributes uniformly throughout the cytoplasm of the cell and seldom forms clusters along the astrocytic processes (Fig. 1*F*). Quantitative analysis shows that GLT-1–GFP fluorescence intensity in the membrane is 38 and 45% higher than that in the cytoplasm in astrocytes and C6 glioma cells, respectively, demonstrating the preferential membrane localization of GLT-1. Interestingly, in ~65% (150 of 271 cells) of transfected astrocytes, long and thin processes are not generated directly from the soma but

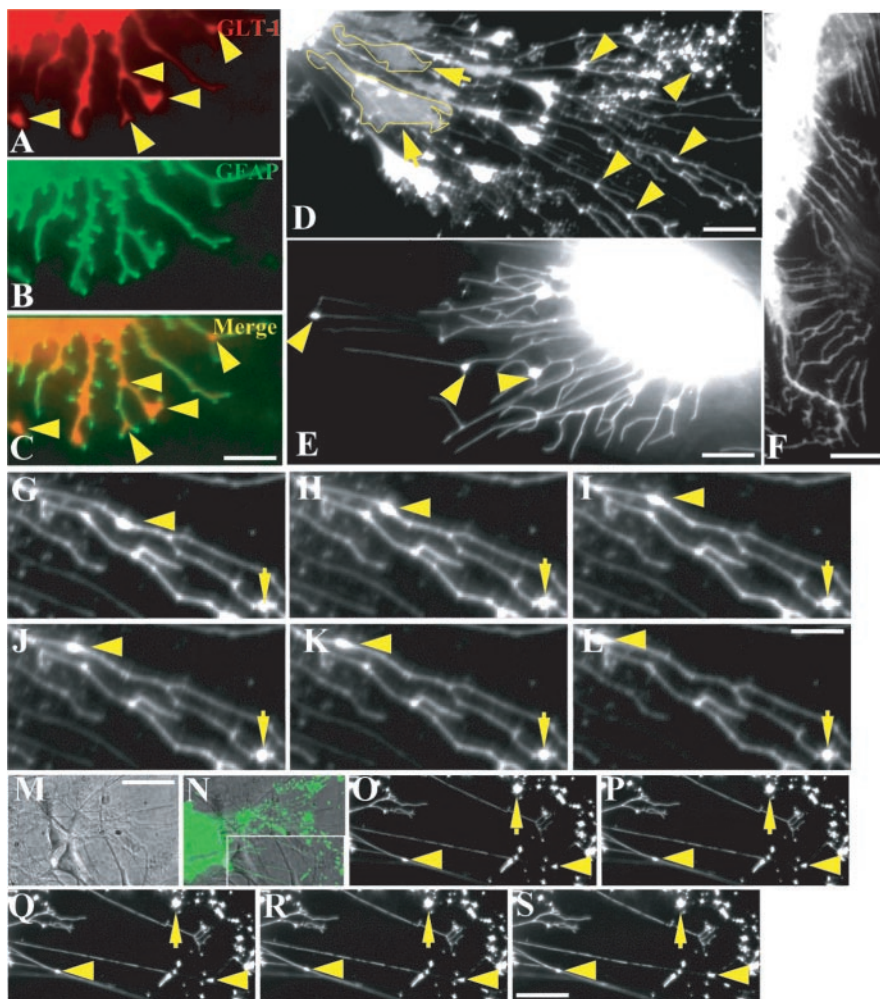


Figure 1. Mobility of GLT-1 clusters in the astrocytic process. Double immunostaining of GLT-1 (*A*) and GFAP (*B*) in astrocyte cultures showing clusters of endogenous GLT-1 in the fork or distal end of the process, as indicated by yellow arrowheads in *A* and the composite image (*C*), is indicated. Astrocytes (*D*) and C6 cells (*E*) transfected with the GFP-tagged GLT-1 expression cassette demonstrate GLT-1 cluster formation, as indicated by yellow arrowheads, whereas expression of GFP alone fails to form clusters (*F*). Please note that some long and thin processes in the astrocyte (*D*) are not generated directly from the cell body but instead from a filopodia-thick structure that is linked with the soma. This structure is outlined in yellow and referred to as a secondary process. Time-lapse imaging of live astrocytes reveals the mobility of GLT-1 clusters in astrocytic processes of both astrocyte cultures alone (*G–L*) and in cocultures with neurons (*O–S*). A differential interference contrast image (*M*) shows the neuron–astrocyte coculture in which the neuron grows on top of an astrocyte expressing GFP-tagged GLT-1. The inset (*N*) outlines the visualized portion of GLT-1 cluster mobility in the neuron–astrocyte coculture. A GLT-1 cluster on the process moves in a retrograde direction, as indicated by the arrowhead, although most of the clusters are stationary, as indicated by arrows. Scale bars: (in *C*) *A–C*, (in *M*) *M*, *N*, 15 μm ; *D*, 10 μm ; *E*, 7 μm ; *F*, (in *S*) *O–S*, 9 μm ; (in *L*) *G–L*, 3 μm .

rather from a protrusion or filopodium linked with the soma (Fig. 1*D*, yellow boxed region). We refer to this structure as a “secondary process” from which thin and long processes are generated and projected. These secondary processes also occurred at a similar frequency in GFP-transfected astrocytes. The average length of an astrocytic process is four to five times longer than that of the soma diameter, leading to a significant area expansion of the membrane. In contrast, mature C6 cells have relatively short processes that usually generate directly from the soma and are approximately equivalent in length to the soma diameter (Fig. 1*E*). GLT-1 clusters in the astrocytic processes have an average area and perimeter of $0.8 \pm 0.04 \mu\text{m}^2$ and $2.6 \pm 0.07 \mu\text{m}$, respectively ($n = 433$), whereas those in C6 cell processes are nearly four times larger in terms of area ($3.1 \pm 0.26 \mu\text{m}^2$; $n = 203$), with a perimeter that is three times longer ($6.5 \pm 0.39 \mu\text{m}$; $n = 203$). With the use of time-lapse fluorescence microscopy, we characterized the

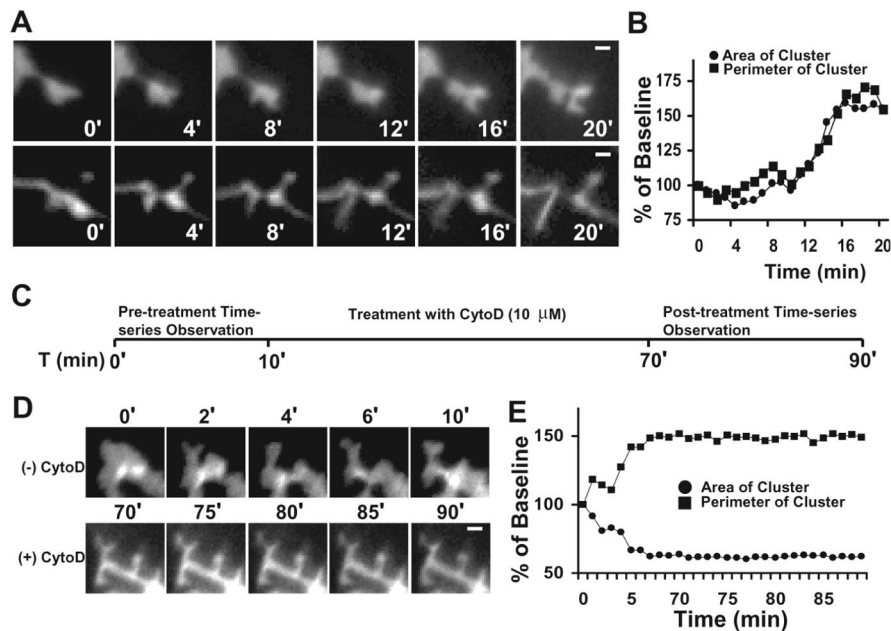


Figure 2. Morphogenesis of the GLT-1 cluster is dependent on the actin network. At the distal end of C6 cell processes, GFP-tagged GLT-1 undergoes rapid morphogenesis. A GLT-1 cluster may split into several smaller clusters (*A*, top), with significant expansion of the membrane area and perimeter (*B*), or disappear when a new process is produced (*A*, bottom). The numbers in *A* and *D* represent time (in minutes). *C*, A schematic showing the experimental protocol for the observation of morphological changes in GLT-1 cluster dimensions before and after CytoD treatment. *D*, Time-lapse images showing morphological changes in the GLT-1 cluster before (top) and after (bottom) CytoD treatment for 60 min. *E*, The quantitation of area and perimeter of a GLT-1 cluster before and after CytoD treatment (10 μ M). Scale bars: *A*, 1.5 μ m; *D*, 1.0 μ m.

mobility of GLT-1 clusters and found that \sim 7% (27 of 433) of GFP-tagged GLT-1 puncta on the shaft of astrocytic processes are bidirectionally mobile with an average speed of 0.5 μ m/min (Fig. 1*G–L*). To further characterize mobility of GLT-1 clusters in a physiological environment and in the absence of dbcAMP, we monitored GLT-1 cluster mobility in neuron–astrocyte cocultures. The coculture of astrocytes with neurons does not change the percentage (18 of 263; 6.8%) or direction of mobile GLT-1 clusters in the astrocytic processes (Fig. 1*M–S*). However, the average speed (0.29 μ m/min) of cluster mobility was reduced in this preparation compared with results obtained from dbcAMP treatment of astrocyte-only cultures.

GLT-1 clusters change in shape and size

In addition to GLT-1 cluster mobility, $>$ 60% (68 of 111) of GLT-1 puncta constantly change their structure in both shape and size at the distal end of both astrocyte and C6 cell processes. To visualize the morphogenesis of GLT-1 clusters, we characterized the clusters on C6 cell processes (four times bigger than clusters in astrocytes). As demonstrated in Figure 2, GLT-1 clusters at the distal end of C6 processes undergo a rapid morphogenesis. A cluster may generate several small clusters (Fig. 2*A*, top) with significant increases in both area and perimeter (Fig. 2*B*) or may be replaced by a newly generated long process (Fig. 2*A*, bottom). Previous studies have demonstrated that actin polymerization and reorganization play an important role in cell motility and microprocess generation (Pollard and Borisy, 2003). Therefore, to investigate the underlying mechanism for the GLT-1 cluster remodeling and quick process generation, C6 cells were treated with cytochalasin D (CytoD), a strong inhibitor of actin polymerization (Tilney et al., 1990; Pollard and Borisy, 2003). Before CytoD treatment, the area of the GLT-1 cluster diminishes to 38% below baseline, whereas the perimeter of the

cluster is augmented 45% above baseline within a 10 min interval (Fig. 2*D,E*), indicating vigorous changes in morphology. After treatment with CytoD for 60 min, however, the area and perimeter undergo only small changes, with a 2% increase in area and a 3% decrease in the perimeter of the cluster within a 20 min recording interval (Fig. 2*D,E*). These results suggest that the morphological changes in GLT-1 clusters at the distal ends of processes are highly dependent on the actin network.

GLT-1 clustering is important in regulating transporter activity

It has been reported that PMA, a phorbol ester analog, quickly decreases GLT-1 activity by inducing rapid GLT-1 internalization, leading to a decrease in the level of the membrane-inserted GLT-1 (Kalandadze et al., 2002). In the present study, treatment with PMA (400 nM) elicits a significant decrease in GLT-1–GFP intensity (Fig. 3*A*, arrow) and a significant increase in the number of GLT-1 clusters (Fig. 3*A*, arrowheads) in the astrocytic processes. This effect occurs 1 min after addition of PMA and reaches a peak \sim 8 min after PMA application (Fig. 3*A*). Quantitative analysis shows that treatment of astrocytes

with PMA induces a $208 \pm 26\%$ [vs $99 \pm 3.14\%$ (control); $n = 7$] and a $199 \pm 25\%$ [vs $101 \pm 11\%$ (control); $n = 7$] increase in the number of GLT-1 clusters above baseline at 8 and 20 min after PMA treatment, respectively. In contrast, although the number of clusters increased after PMA treatment, there is no significant change in GLT-1 cluster intensity. Interestingly, GLT-1–GFP internalization also occurred within the secondary processes. Approximately 28% of astrocytes (two of seven) demonstrated a significant accumulation of GLT-1 in the secondary processes (Fig. 3*E*). Before PMA addition, most of the GLT-1 is located in the membrane of the secondary processes (time, 0 min) (Fig. 3*E*). Addition of PMA elicits an immediate aggregation of cytoplasmic GLT-1 and a corresponding depletion of GLT-1 in the membrane of the secondary process (Fig. 3*E*).

To determine whether GLT-1 internalization induced by PMA preferentially occurs in the astrocytic processes, we measured the change in GLT-1 intensity in the soma membrane of several astrocytes that do not bear long and thin processes after PMA addition. The GLT-1 intensity in the soma membrane after PMA treatment showed no significant difference (9% decrease within 20 min; $n = 5$) (Fig. 3*D*) compared with no treatment (control, 3% decrease), demonstrating that PMA (400 nM) treatment basically has no effect on GLT-1 trafficking in the astrocytic soma membrane. Pretreatment with the nonselective PKC inhibitor bisindolylmaleimide II (Bis II) significantly inhibits the PMA-induced new generation of GLT-1 clusters (5% decrease from baseline levels within 20 min; $n = 5$) (Fig. 3*B*), suggesting that PKC activation is required for PMA-induced GLT-1 internalization.

For additional confirmation of this point, immunoblots were used to determine the change in total membrane-inserted GLT-1 protein (including the membranes of soma, secondary processes, and long and thin processes). Western blot analysis demonstrates

that there are no changes in total GLT-1 protein after treatment with PMA, Bis II, or PMA and Bis II in combination (Fig. 4A). In contrast, PMA application induces a 47% decrease in the total membrane-inserted GLT-1 immunoreactivity, whereas Bis II pretreatment basically restores the membrane-inserted GLT-1 immunoreactivity to >85% of control (Fig. 4A). Because PMA fails to induce any significant change in GLT-1 in the astrocytic soma membrane, it is reasonable to conclude that the PMA-induced 47% decrease in total membrane-inserted GLT-1 basically results from GLT-1 internalization in the primary and secondary astrocytic processes. To further verify the nature of GLT-1 trafficking in the astrocytic process, 0.4 M sucrose, a strong inhibitor of clathrin (Jarousse and Kelly, 2000), was incubated with the astrocyte cultures for 45 min. After this hypertonic treatment, addition of PMA failed to induce the generation of new GLT-1 clusters in the astrocytic processes (108 ± 4.3 and $99 \pm 2.6\%$ of the baseline at 10 and 20 min, respectively; $n = 7$) (supplemental Figure 1, available at www.jneurosci.org). Because high-molarity sucrose also may have other effects on the cell in addition to the inhibition of clathrin, we also introduced a cDNA encoding a dominant-negative form of dynamin (Conner and Schmid, 2003) into astrocytes by cotransfection with pEGFP-GLT-1. Expression of K44A, which inhibits endocytic vesicle formation, prevented PMA-induced generation of GLT-1 clusters in the astrocytic process (96 ± 4.4 and $93 \pm 3.2\%$ of baseline at 10 and 20 min, respectively; $n = 13$) (Fig. 3C). Together, these data suggest that the generation of new GLT-1 clusters in the astrocytic processes results from clathrin-dependent GLT-1 internalization.

To determine the relationship between GLT-1 trafficking in the processes and glutamate transporter activity, GLT-1 glutamate transport capacity was determined in both stably transfected C6 cells (Fig. 4B) and astrocytes (Fig. 4C). To isolate the specific GLT-1 activity, a selective GLT-1 inhibitor, dihydrokainate (DHK; 500 nM), was included in the uptake assay to block GLT-1 activity. By comparing the glutamate uptake in the presence or absence of DHK, we calculated the specific GLT-1 activity. Consistent with the above findings, PMA treatment for 10 min significantly reduced GLT-1 activity to 55% of control ($p < 0.01$) (Fig. 4B,C) in both the stably transfected C6 cells and cultured astrocytes. Pretreatment with either Bis II or high sucrose (0.4 M) significantly inhibited the PMA-induced decrease in GLT-1 activity (Fig. 4B–D), suggesting that both PKC activity and clathrin-dependent endocytosis are required for the PMA-induced decrease in GLT-1 activity.

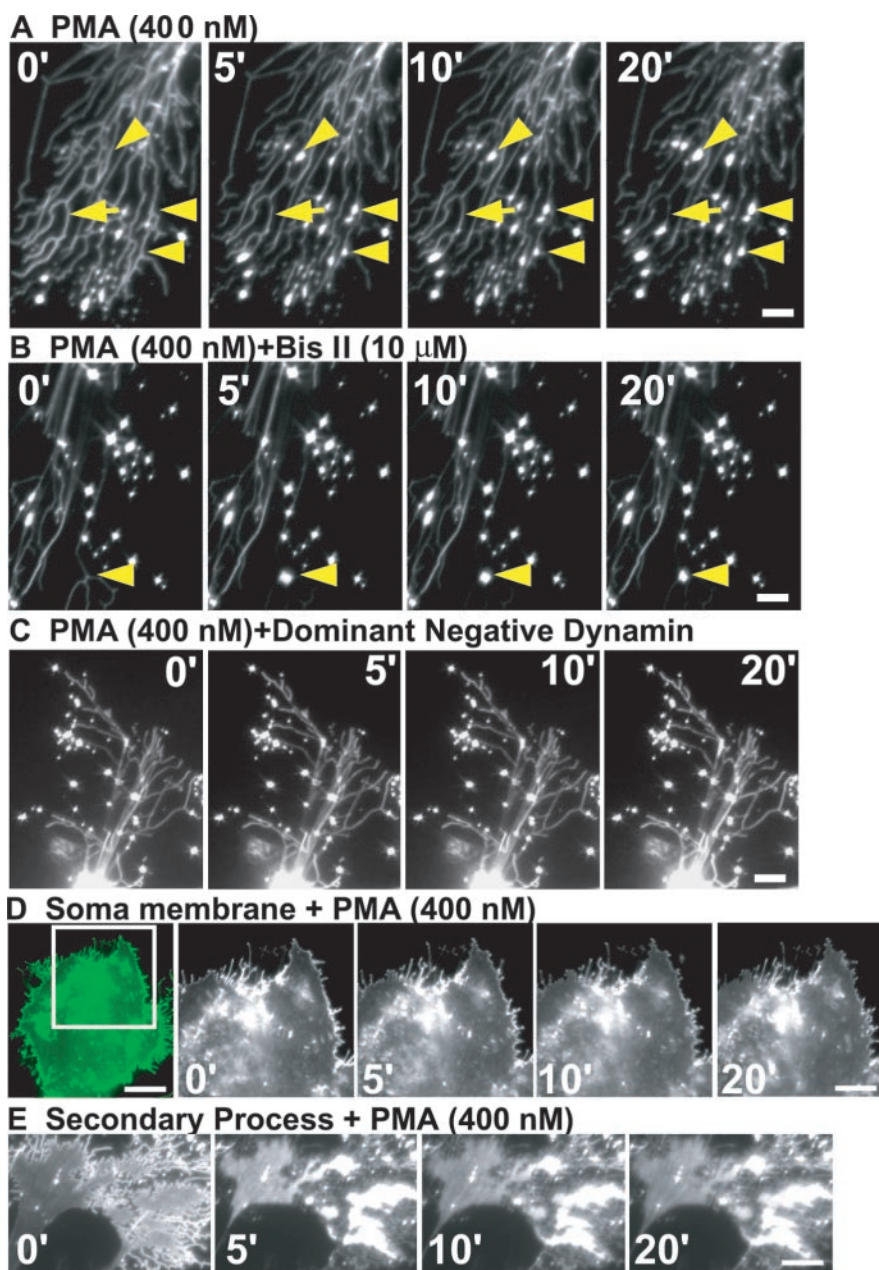


Figure 3. PMA treatment preferentially reduces the level of GLT-1 protein in astrocytic process. Representative time-series pictures show changes in GLT-1 intensity and clusters in the astrocytic processes after treatments with 400 nM PMA (*A*), 400 nM PMA and 10 μM Bis II in combination (*B*), and 400 nM PMA on a dominant-negative dynamin-expressing astrocyte (*C*). The arrowheads in *A* and *B* outline the appearance of new clusters. *D*, Time-series pictures showing changes in GLT-1 intensity associated with the soma membrane after treatment with PMA (400 nM). The inset to the left outlines the visualized portion of the astrocyte. *E*, Time-series pictures showing changes in GLT-1 intensity after treatment with PMA (400 nM) on the astrocytic secondary process. Quantitations are based on five to nine independent experiments. The numbers in *A–E* represent time (in minutes). Scale bars: *A*, *C*, 5 μm; *B*, 10 μm; *D*, 25 μm (left image) and 15 μm (other 4 images); *E*, 8 μm.

Discussion

It is the astrocytic process and not the soma that directly contacts the neuronal synapse, and it is this association that is believed to be crucial for regulating the glutamate concentration at the synaptic cleft. The present study provides direct evidence that the GLT-1 clusters in the astrocytic processes play an important role in regulating GLT-1 activity. It has been reported that the neuronal GABA transporter 1 associates with clathrin and dynamin to undergo a rapid internalization and insertion recycling process (Deken et al., 2003). GLT-1 clusters identified in the present

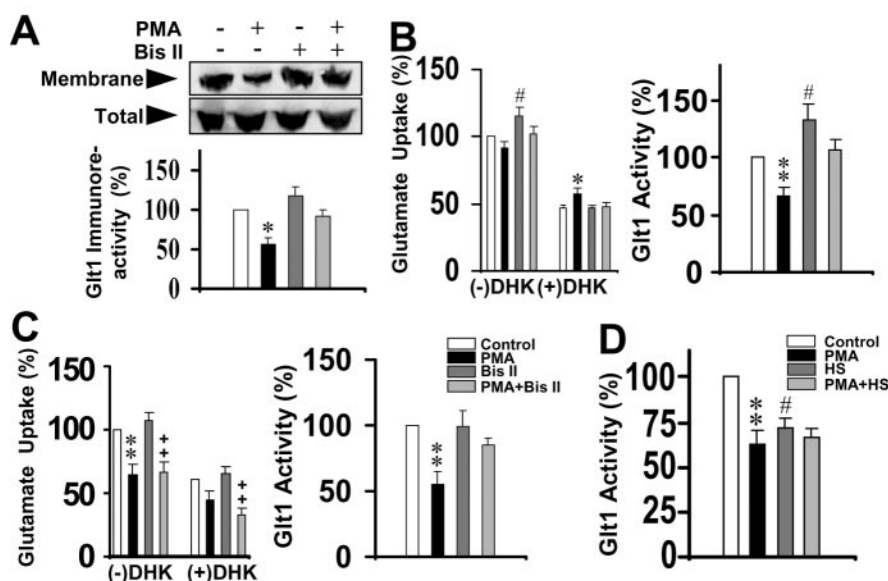


Figure 4. PMA treatment decreases GLT-1 activity. *A*, A representative immunoblot (top) showing the redistribution of GLT-1 in the membrane after treatments with 400 nM PMA, 10 μ M Bis II, or a combination of both. The bar graph (bottom) summarizes changes in GLT-1 immunoreactivity after treatment with PMA, Bis II, or both. * p < 0.01, compared with control. Control values are measured in the absence of PMA or Bis II. Mean \pm SE; n = 4. *B*, Quantitation of glutamate uptake in the presence or absence of DHK (500 nM) (left) and GLT-1-specific (right) glutamate uptake after treatment with PMA, Bis II, or both in C6 cells stably expressing GFP-tagged GLT-1. Mean \pm SE; * p < 0.05; ** p < 0.01; # p < 0.05, compared with control; n = 9. *C*, Quantitation of glutamate uptake in the presence or absence of DHK (500 nM) (left) and GLT-1-specific (right) glutamate uptake after treatment with PMA, Bis II, or both in primary astrocyte cultures. Mean \pm SE; ** p < 0.01, compared with control; + p < 0.01, compared with Bis II; n = 9. *D*, Quantitation of GLT-1-specific activity after treatment with PMA (400 nM), high sucrose (0.4 M), or PMA and high sucrose in combination in C6 cells stably expressing GFP-tagged GLT-1. Mean \pm SE; ** p < 0.01; # p < 0.05, compared with control; n = 6.

study may also be an accumulation of clathrin-wrapped vesicles, providing a mechanism by which GLT-1 traffics along the process to the soma for degradation or recycling. It has been suggested that the presence of GLT-1 in astrocytic processes enables the cell to sense the change in glutamate level, thereby providing a mechanism for accumulation of GLT-1 along certain parts of the membrane where higher glutamate removal is required (Chaudhry et al., 1995). To accomplish this level of regulation, GLT-1 in the process membrane may recycle by an internalization–insertion mechanism, and GLT-1 clusters may therefore act as an internal reserve of transporter molecules. An astrocytic process can also form a close interaction with the presynaptic zone of a neuronal axon (Minelli et al., 2001), thereby raising the possibility that GLT-1 cluster mobility is important for rapid translocation of GLT-1 to the astrocyte–neuronal synaptic site.

It has been reported that the dendritic spine undergoes a dramatic change in shape in primary neuronal cultures transfected with GFP-tagged actin (Fischer et al., 1998), revealing a rapid actin-based plasticity of the dendritic spine. Similarly, at the distal end of C6 processes, we also identified a dynamic change in filopodia-like structures and a rapid actin-based plasticity of GLT-1 clusters. The morphogenesis of the GLT-1 cluster may result from a simple GLT-1 redistribution to the neighboring membrane or from new generation or reorganization of the membrane, to which GLT-1 is then translocated. Because CytoD treatment freezes the morphology of GLT-1 clusters, our data suggest that the morphogenesis of GLT-1 clusters is a result of reorganization or new generation of the membrane driven by the actin dynamics, rather than simple redistribution. Interestingly, CytoD treatment significantly changes GLT-1 cluster morphology and leads to the generation of new processes originating from

the soma (data not shown), suggesting that the actin network is important for the regulation of astrocytic process sprouting.

In the present study, PMA treatment induces a preferential internalization in the astrocytic processes that is then inhibited by pretreatment with a high concentration of sucrose (0.4 M) or expression of a dominant-negative form of dynamin, suggesting that PMA treatment is coupled with clathrin-dependent GLT-1 endocytosis. The newly formed GLT-1 clusters are believed to be generated *de novo* by the aggregation and internalization of GLT-1 molecules inserted in the process membrane, because GLT-1 intensity is diminished in the vicinity where new GLT-1 clusters are produced. Thus far we cannot explain why PMA-induced GLT-1 internalization selectively occurs in the process and not the cell body. PMA is a phorbol ester that is reported to bind specifically with C1 domain-containing proteins such as classical and novel PKCs (Zhou et al., 2003) and synaptic adhesion molecules such as Munc 13 and Munc 18 (Jahn and Sudhof, 1999). It is possible that certain types of PKC may preferentially localize within the astrocytic process, thereby preferentially generating a PMA response for GLT-1 transporters localized on the astrocytic process. In addition to GLT-1 traf-

ficking, PMA treatment also leads to a significant decrease in GLT-1 activity that is prevented by pretreatment with either Bis II or high sucrose (0.4 M), suggesting that the clathrin-dependent GLT-1 trafficking in the astrocytic processes plays a very important role in the regulation of glutamate uptake. Interestingly, hypertonic treatment alone significantly decreases GLT-1 activity to 70% of control values (Fig. 4*D*). Because high sucrose is able to block the clathrin-dependent endocytosis (Jarousse and Kelly, 2000), it is reasonable to speculate that GLT-1 internalization itself is an alternative pathway for removal of glutamate from the synapse. Together, we conclude that GLT-1 trafficking in astrocytic processes plays an important role in regulating GLT-1 activity. Because astrocytic processes (and not the soma) contact the neuronal synapse and maintain the glutamate level in the synaptic cleft, GLT-1 trafficking in astrocyte processes could provide an important and dynamic mechanism for maintaining the local glutamate concentration at the synapse.

References

- Auger C, Attwell D (2000) Fast removal of synaptic glutamate by postsynaptic transporters. *Neuron* 28:547–558.
- Chaudhry FA, Lehre KP, van Lookeren Campagne M, Ottersen OP, Danbolt NC, Storm-Mathisen J (1995) Glutamate transporters in glial plasma membranes: highly differentiated localizations revealed by quantitative ultrastructural immunocytochemistry. *Neuron* 15:711–720.
- Conner SD, Schmid SL (2003) Regulated portals of entry into the cell. *Nature* 422:37–44.
- Conti F, Weinberg RJ (1999) Shaping excitation at glutamatergic synapses. *Trends Neurosci* 22:451–458.
- Deken SL, Wang D, Quick MW (2003) Plasma membrane GABA transporters reside on distinct vesicles and undergo rapid regulated recycling. *J Neurosci* 23:1563–1568.

- Fagg GE, Foster AC (1983) Amino acid neurotransmitters and their pathways in the mammalian central nervous system. *Neuroscience* 9:701–719.
- Fischer M, Kaech S, Knutti D, Matus A (1998) Rapid actin-based plasticity in dendritic spines. *Neuron* 20:847–854.
- Hughes EG, Maguire JL, McMinn MT, Scholz RE, Sutherland ML (2004) Loss of glial fibrillary acidic protein results in decreased glutamate transport and inhibition of PKA-induced EAAT2 cell surface trafficking. *Brain Res Mol Brain Res* 124:114–123.
- Jahn R, Sudhof TC (1999) Membrane fusion and exocytosis. *Annu Rev Biochem* 68:863–911.
- Jarousse N, Kelly RB (2000) Selective inhibition of adaptor complex-mediated vesiculation. *Traffic* 1:378–384.
- Kalandadze A, Wu Y, Robinson MB (2002) Protein kinase C activation decreases cell surface expression of the GLT-1 subtype of glutamate transporter. Requirement of a carboxyl-terminal domain and partial dependence on serine 486. *J Biol Chem* 277:45741–45750.
- Minelli A, Barbaresi P, Reimer RJ, Edwards RH, Conti F (2001) The glial glutamate transporter GLT-1 is localized both in the vicinity of and at distance from axon terminals in the rat cerebral cortex. *Neuroscience* 108:51–59.
- Pollard TD, Borisy GG (2003) Cellular motility driven by assembly and disassembly of actin filaments. *Cell* 112:453–465.
- Robinson MB (1998) The family of sodium-dependent glutamate transporters: a focus on the GLT-1/EAAT2 subtype. *Neurochem Int* 33:479–491.
- Rothstein JD, Dykes-Hoberg M, Pardo CA, Bristol LA, Jin L, Kuncl RW, Kanai Y, Hediger MA, Wang Y, Schielke JP, Welty DF (1996) Knockout of glutamate transporters reveals a major role for astroglial transport in excitotoxicity and clearance of glutamate. *Neuron* 16:675–686.
- Schlag BD, Vondrasek JR, Munir M, Kalandadze A, Zelenka OA, Rothstein JD, Robinson MB (1998) Regulation of the glial Na⁺-dependent glutamate transporters by cyclic AMP analogs and neurons. *Mol Pharmacol* 53:355–369.
- Sutherland ML, Delaney TA, Noebels JL (1995) Molecular characterization of a high affinity mouse glutamate transporter. *Gene* 162:271–274.
- Sutherland ML, Delaney TA, Noebels JL (1996) Glutamate transporter mRNA expression in proliferative zones of the developing and adult murine CNS. *J Neurosci* 16:2191–2207.
- Tanaka K, Watase K, Manabe T, Yamada K, Watanabe K, Takahashi K, Iwana H, Nishikawa T, Ichihara N, Kikuchi T, Okuyama S, Kawashima N, Hori S, Takimoto M, Wada K (1997) Epilepsy and exacerbation of brain injury in mice lacking the glutamate transporter GLT-1. *Science* 276:1699–1702.
- Tilney LG, Connelly PS, Portnoy DA (1990) Actin filament nucleation by the bacterial pathogen, *Listeria monocytogenes*. *J Cell Biol* 111:2979–2988.
- Trotti D (2002) A role for glutamate transporters in neurodegenerative diseases. *Adv Exp Med Biol* 513:225–248.
- Xu NJ, Bao L, Fan HP, Bao GB, Pu L, Lu YJ, Wu CF, Zhang X, Pei G (2003) Morphine withdrawal increases glutamate uptake and surface expression of glutamate transporter GLT1 at hippocampal synapse. *J Neurosci* 23:4775–4784.
- Zhou J, Fariss RN, Zelenka PS (2003) Synergy of epidermal growth factor and 12(*S*)-hydroxyeicosatetraenoate on protein kinase C activation in lens epithelial cells. *J Biol Chem* 278:5388–5398.